ISSN: 1410-8917
Jurnal Kimia Sains & Aplikasi
e-ISSN: 2597-9914

Jurnal Kimia Sains dan Aplikasi 23 (12) (2020): 440–448

Jurnal Kimia Sains dan Aplikasi
Journal of Scientific and Applied Chemistry

Journal homepage: http://ejournal.undip.ac.id/index.php/ksa

Preparation of Composite Derived from Banana Peel Activated Carbon and $MgFe_2O_4$ as Magnetic Adsorbent for Methylene Blue Removal

Arie Hardian [a,1,*], Rosi Rosidah [a], Senadi Budiman [a], Dani Gustaman Syarif [b,2,*]

[a] Department of Chemistry, Faculty of Sciences and Informatics, Universitas Jenderal Achmad Yani, Cimahi, Indonesia
[b] Center for Applied Nuclear Science and Technology (PSTNT), National Nuclear Energy Agency (BATAN), Bandung, Indonesia

*Corresponding author: (1) arie.hardian@lecture.unjani.ac.id; (2) danigus@batan.go.id

https://doi.org/10.14710/jksa.23.12.440-448

Article Info

Article history:

Received: 25th November 2020
Revised: 13th January 2021
Accepted: 31th January 2021
Online: 31st January 2021

Keywords:
activated carbon; banana peel; magnetic adsorbent; methylene blue; $MgFe_2O_4$

Abstract

Methylene blue (MB) is one of the dyes used often by the textile industry. Therefore, MB residual is contained in the textile industry waste. MB can irritate, leading to permanent eye and animal injuries; therefore, the textile industry waste concentration must be degraded before disposed to the environment. MB residual in textile industry waste can be treated with activated carbon adsorption. However, the adsorption method is less effective because the deposition takes a long time. This research aims to make activated carbon composites from banana peels and magnesium ferrite (BPAC/$MgFe_2O_4$) using the coprecipitation method to obtain activated carbon with magnetic properties (magnetic adsorbent). The obtained composite was characterized using X-Ray Diffraction (XRD), Scanning Electron Microscope (SEM), Energy Dispersive X-Ray (EDX), and Surface Area Analyzer. The adsorption performance of methylene blue on composites was evaluated with variations in pH, concentration, contact time, determination of adsorption isotherms, and kinetics of adsorption. XRD analysis results showed the composite has a cubic crystal structure with a crystallite size of 7.69 nm. SEM analysis results show the surface morphology has pores with irregular shapes. EDX analysis results showed that the composition of activated carbon composite was 65.56% carbon, 2.28% Mg, 5.50% Fe, and 26.66% O. The results surface area analysis showed a composite surface area of 88.134 m^2/g. Composite adsorption performance showed maximum results at pH 7, variations in concentration at 10 ppm, and contact time 180 minutes with adsorption capability of 99.26%. Determination of the adsorption isotherm follows the Freundlich adsorption isotherm model with a pseudo-second-order adsorption kinetics model. The obtained BPAC/$MgFe_2O_4$ composite can potentially be a magnetic adsorbent capable of adsorbing methylene blue in an aqueous solution.

1. Introduction

The textile industry has a significant role in Indonesia. The industrial sector plays an essential role in promoting economic growth, poverty alleviation, and creating job opportunities to reduce high levels of unemployment [1]. Nevertheless, behind the positive impact that the textile industry has, there are negative impacts it causes. One of the negative impacts is the waste produced. The waste is not environmentally friendly and harmful to health.

The types of dyes used in the textile industry today are very diverse. Therefore, textile waste handling becomes very complicated and requires several steps until it is entirely safe to be released into the aquatic environment [2]. Methylene blue (MB) is a water-soluble organic dye and is widely used in the textile industry but can cause irritation, leading to permanent eye and animal injuries [3].

Many techniques or methods are used to be able to adsorb dyes in the textile industry, one of which is the

adsorption method using adsorbents. Activated carbon can be used as a bleaching agent (dye remover), gas absorber, and metal absorber [4]. The adsorption method using adsorbents alone turned out to be less effective because the deposition only relies on the force of gravity alone. In recent years research has developed on adsorbent composites with magnetic materials that can be easily separated from the dye waste solution in the adsorption process by utilizing an external magnetic field. Magnetic separation has become one of the most promising water purification techniques in the environment. Its nature does not produce contaminants such as flocculants and can filter or separate large amounts of waste in a short time [5].

Banana is a fruit that is easy to grow in tropical countries such as Indonesia. Therefore, a banana is one of the fruits abundant in Indonesia. After harvesting bananas, 80% of the peels, stems, and leaves are removed without further processing. This has resulted in an immense enough potential for banana peel waste so that it is necessary to overcome the banana peel to have more use value [6]. LFX *et al.* [7] has conducted previous research that banana peels can be used as adsorption on azo dyes.

In recent years, the spinel ferrite (SFs) nanoparticles have been a fascinating research object and have become the focus of many kinds of research for both scientific and technological interests. The SFs nanoparticles have the structural formula MFe_2O_4 (M is a divalent metal ion, such as Ni, Co, Cu, Mn, Mg, Zn, Fe) with a cubic spinel crystal structure [8]. Magnesium ferrite nanoparticles attract many researchers' attention due to their low toxicity [9], high chemical stability [10], and high saturation magnetization value [11, 12]. Spinel ferrite is commonly used as a magnetic adsorbent for any kind of pollutants such as ion metals, dyes, and other such as phenol, tetracycline, and phosphorous compounds [13]. Tang *et al.* [14] reported that doping ~10% magnesium into α-Fe_2O_3 could increase the specific surface area from 162 m^2/g to 438 m^2/g, which is 2.7 times higher. Therefore, increase the adsorption performance of particles toward As(III) and As(V) from aqueous solutions. Substitution of a lighter metal ion Mg^{2+} into heavy Fe^{3+} in α-Fe_2O_3 induces internal and surface defects/pores, lead to increasing the surface area of $Mg_{0.27}Fe_{2.50}O_4$. The magnetic properties of $MgFe_2O_4$ depend on its structure, such as particle size, crystallinity, crystallite size, and cation distribution. Modification toward $MgFe_2O_4$ structure can be done by choosing a suitable synthesis method. There are many reports on magnetic properties of $MgFe_2O_4$ with different synthesize method, e.g., sol-gel/combustion method produced 30.6 emu/g [15], ceramic method plus mechanical milling produced 36 emu/g [16], one-step mechanochemical route produced 50 emu/g [17], and ultrasonic wave assisted ball milling produced 54.84 emu/g [12].

Although magnesium ferrite can adsorb pollutants in an aqueous solution, this adsorbent's development prepares its composite with a common adsorbent such as activated carbon (AC). Kaur *et al.* [18] reported that a nanocomposite of $MgFe_2O_4$-loaded activated charcoal was prepared in a sol-gel approach with a high Cr(VI) sorption capacity of 500 mg/g at pH 2.0. Based on our literature research, there is still a lack of information toward synthesis and characterization of AC from banana peels (BPAC) and magnesium ferrite composite, also its performance as an adsorbent for methylene blue (MB) removal. In this work, we reported a simple method in preparation BPAC/$MgFe_2O_4$ composites and its adsorption performance study (optimum condition, isotherm, and kinetic) as an adsorbent for MB removal in an aqueous solution.

2. Methodology

This research went through several experimental stages using the equipment and materials described as follows.

2.1. Equipment/ Tool/ Material.

The equipment used includes glassware, porcelain cups, analytical balances, hot plate, magnetic stirrer, oven, furnace, 100 mesh size sieve, and external magnet. The instruments used were Mettler Toledo Analytical Balance, Mettler Toledo pH meters, Hotplate magnetic stirrer IKA 381000X, X-Ray Diffraction Bruker D8 Advance, Scanning Electron Microscope JSM-6390LV, Surface Area Meter Quantachrome, Energy Dispersive X-ray HITACHI, and Spectrophotometer UV Vis Genesys 10s. The materials used were Kepok banana peels, MgCl2.6H2O (Aldrich, 99.995% trace metal basis), FeCl3.6H2O (Aldrich, ≥ 99% p.a.), NH4OH, NaCl, methylene blue, and distilled water.

2.2. Preparation of activated carbon composites from banana peels and $MgFe_2O_4$ (BPAC/ $MgFe_2O_4$)

The banana peel was washed first and cut into small pieces, then dried under the sun for three days. Furthermore, the dried banana peel was burned in a furnace at 300°C for 15 minutes. Banana peel that has become carbon cooled in a desiccator then sieved with a 100-mesh sieve. Carbon from the banana peel was chemically activated using 1% NaCl solution, stirring for 120 minutes using a 500-rpm magnetic stirrer at 80°C. Then filtered and washed to a neutral pH and dried at 105°C.

The obtained activated carbon was then composited with magnesium ferrite ($MgFe_2O_4$) using the coprecipitation method [11]. Magnesium ferrite is made from 1.00-gram $MgCl_2.6H_2O$ (Aldrich, 99.995% trace metal basis) and 2.70 grams $FeCl_3.6H_2O$ (Aldrich ≥99% p.a.) as a provider of Mg^{2+} and Fe^{3+} ions and added with 50 mL of distilled water. Then added 1.50 grams of activated carbon from banana peels and added 2 M NH_4OH solution slowly while stirring until a black precipitate was formed. The composite was then filtered and washed to neutral pH, dried at 105°C for 120 minutes, and calcined at 500°C for 60 minutes. The obtained composite was then characterized using *X-Ray Diffraction* Bruker D8 Advance, *Scanning Electron Microscope* JSM-6390LV, *Surface Area Analyzer Quanta chrome* dan *Energy Dispersive X-Ray* HITACHI.

2.3. Performance Test of BPAC/$MgFe_2O_4$ Composite Adsorption on Methylene Blue with Optimization of pH, Variation of Contact Time, and Concentration

The primary solution was made of methylene blue in 100 ppm, then diluted to produce a series of standard MB solutions consist of 5 ppm, 10 ppm, 20 ppm, 30 ppm, 40 ppm, and 50 ppm. The absorbance was then measured using a spectrophotometer—a standard curve by plotting the concentration against the absorbance. Figure 1 showed the linear regression of the standard curve of MB solutions.

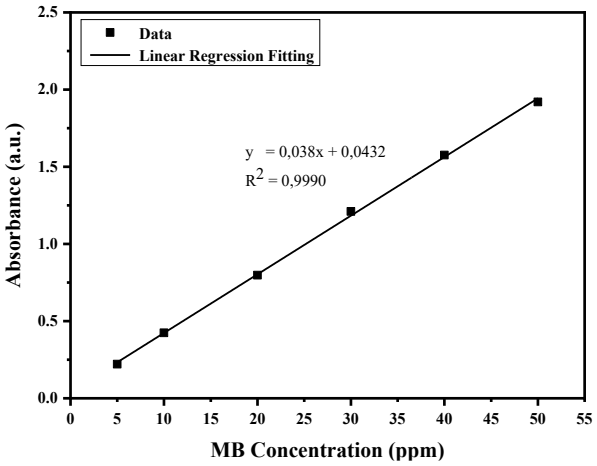

Figure 1. Standard curve of methylene blue solutions

According to the data collection carried out, the main solution was diluted. There were three parameters or variables to study the absorbance performance: the concentration of MB in aqueous solution, pH solution, and contact time between adsorbent and adsorbate. Five concentrations were chosen for concentration variation, which is 10, 15, 20, 25, and 30 ppm. For pH variation, the pH of MB solution at a middle concentration (20 ppm) was varied with three different pH which are 5, 7, and 9 representatives for acid, neutral, and base environment, respectively. For contact time variation, decreasing MB concentration was monitored for 3 hours of contact with composite while stirred using a magnetic stirrer.

The data collection process began by preparing 20 mL of methylene blue into a beaker and adding 0.01 grams of BPAC/$MgFe_2O_4$ composites. Then stirred at a speed of 300 rpm using a magnetic stirrer, carried out for 60 minutes to find an optimum condition in adsorbate concentration, pH, and contact time. After stirring using a magnetic stirrer, it is stored on an external magnet to separate the composite within 2 minutes. The absorbance was measured using the UV Vis Spectrophotometer.

Methylene blue, whose absorbance has been measured using a UV Vis spectrophotometer at 663 nm wavelength, was entered into a linear regression of the calibration curve for methylene blue's standard solution. Then the percentage of removal was obtained by entering the concentration of methylene blue into equation (1) [19]:

$$\% \text{ removal} = \frac{Co-Ce}{Co} x\ 100\ \% \qquad (1)$$

Note:

Co = Initial concentration of methylene blue

Ce = Equilibrium concentration of methylene blue

3. Result and Discussion

Characterization of BPAC/$MgFe_2O_4$ composites and the adsorption performance of BPAC/$MgFe_2O_4$ composites against methylene blue was carried out using UV-Vis Spectrophotometry with various tests. The variations made were variations in pH, contact time, and MB concentration. The adsorption isotherms were determined using Langmuir isotherm and Freundlich isotherms, then determined adsorption kinetics using pseudo-first-order and pseudo-second-order.

3.1. Magnetic Properties of Composites BPAC/$MgFe_2O_4$

The BPAC/$MgFe_2O_4$ composites' magnetic properties were tested using an external magnet. This was done to determine how strongly the composite can respond or be attracted by a magnet.

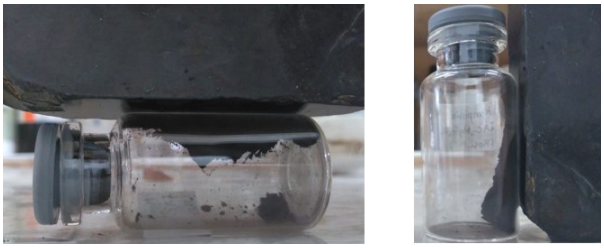

Figure 2. Magnetic properties response test of composites BPAC/$MgFe_2O_4$ toward the external magnetic field

Based on Figure 2, the BPAC/$MgFe_2O_4$ composite's ability to respond to a magnetic field was excellent. This was proved by the black composite powder's attraction attached to the bottle with a magnet. This magnetic property comes from magnesium ferrite ($MgFe_2O_4$). This good magnetic response capability facilitates the separation of composites in an aqueous medium. This process was used to separate the composites after methylene blue adsorption by storing them on an external magnet for 2 minutes approximately (Figure 3). In this separation process, the filtration process can be minimized using filter paper.

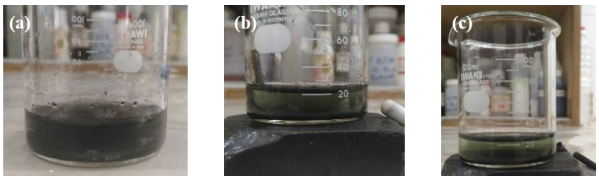

Figure 3. The separation process of BPAC/$MgFe_2O_4$ composites with methylene blue using external magnets. (a) After the adsorption process, (b) The methylene blue solution was suspended on an external magnet; (c) the methylene blue solution after standing for 2 minutes on an external magnet

3.2. Characterization of Composites BPAC/$MgFe_2O_4$ by X-Ray Diffraction (XRD)

X-ray diffraction pattern of the obtained BPAC/$MgFe_2O_4$ composite is shown in Figure 4.

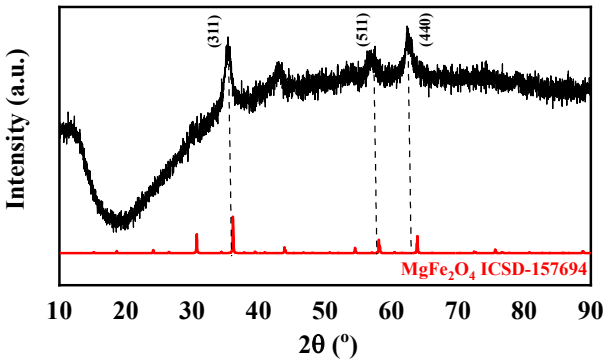

Figure 4. X-ray diffraction pattern of composites BPAC/$MgFe_2O_4$ produced by the coprecipitation method.

The X-ray diffraction pattern shown in Figure 4 shows the relative intensity of the highest peaks appearing in the X-ray diffraction pattern of the obtained $MgFe_2O_4$ matches with ICSD-157694. The XRD characterization results showed that $MgFe_2O_4$, with the principal peak in the 2θ region around 35° was the diffraction peak (311). Other peaks identified in the sample are (511) and (440), which crystallize in the cubic crystal system. These results were consistent with those reported by Suharyadi *et al.* [20] on the synthesis of $MgFe_2O_4$ through the coprecipitation method showing diffraction peaks at (311), (511), and (440). The crystallite size was calculated using the Scherrer equation shown in equation (2).

$$D = \frac{k.\lambda}{\beta \cos\theta} \quad (2)$$

where D is crystallite size, λ = 0.154060 nm is the Cu-Kα X-ray wavelength, β is the Full Width and Half Maximum (FWHM) value of each characterization peak, θ is diffraction angle, and k=0.9 is a constant [21].

Table 1. Crystallite size of $MgFe_2O_4$ in composites BPAC/$MgFe_2O_4$ using the Scherrer approach

θ (deg)	θ (rad)	Cos θ	FWHM (deg)	FWHM (rad)	D (nm)
17.71	0.31	0.95	1.16	0.02	7.28
31.18	0.54	0.86	1.13	0.02	8.10
Average crystallite size					7.69

The crystallite size obtained (Table 1) was following the percentage of crystallinity obtained. The percentage of crystallinity (%crystallinity) obtained was 10.9%, and the amorphous percentage was 80.9%. The %crystallinity (or ratio of crystalline to non- or nano-crystalline species in a material) is evaluated by evaluating the baseline to peak separation in an extended scan range. The small crystallite size was obtained due to the addition of activated carbon. According to Aflahannisa and Astuti [22], research is reported as a decrease in crystallite size and an increase in carbon mass.

3.3. Characterization of Composites BPAC/$MgFe_2O_4$ by Scanning Electron Microscope (SEM)

Figure 5 shows the BPAC/$MgFe_2O_4$ particles' surface morphology analyzed using SEM. The characterization results of the BPAC/$MgFe_2O_4$ composite shown in Figure 5a that the sample's surface morphology has pores with irregular shapes. In Figure 5b, it can be seen that the sample was heterogeneous or non-uniform.

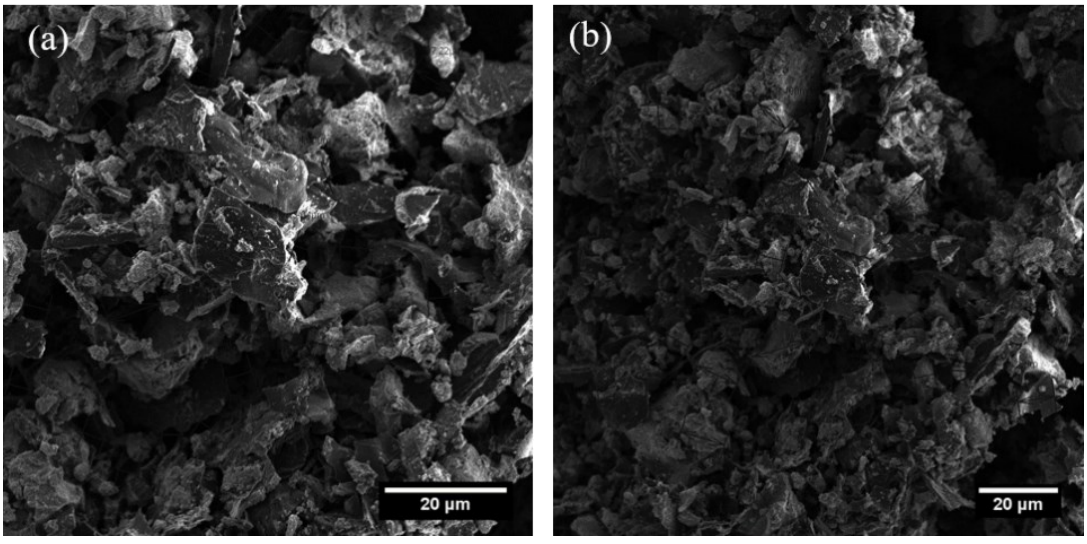

Figure 5. Surface morphology of BPAC/$MgFe_2O_4$ composite using a Scanning Electron Microscope

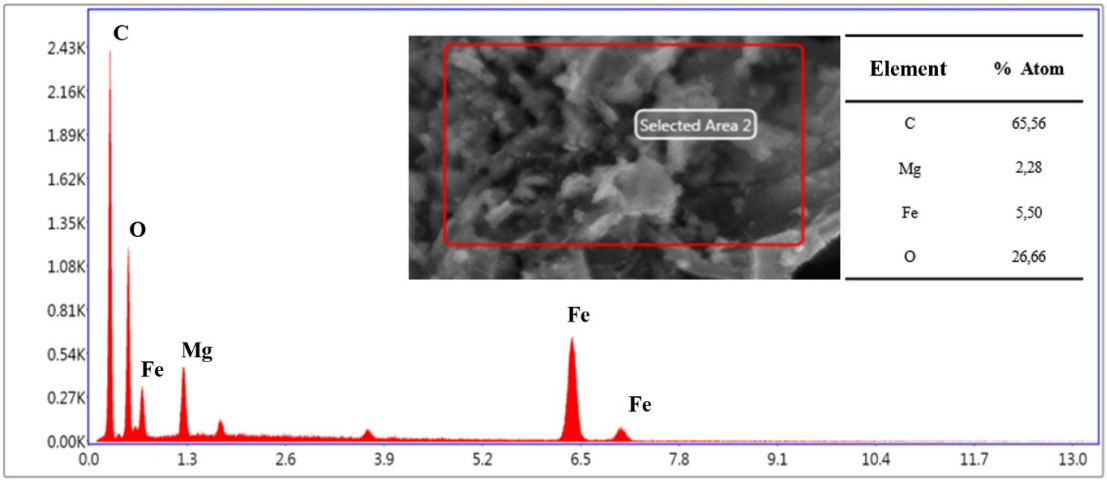

Figure 6. Elemental composition of BPAC/$MgFe_2O_4$ composite using EDX

3.4. Characterization of Composites BPAC/$MgFe_2O_4$ by Energy Dispersive X-Ray Spectroscopy (EDX)

The composition and levels of elements in the BPAC/$MgFe_2O_4$ composites were analyzed using EDX. The main content of activated carbon from banana peels and $MgFe_2O_4$, respectively, can be seen in Figure 6. The composition of the obtained composite was 65.56% carbon (C), 2.28% magnesium (Mg), 5.50% iron (Fe), and 26.66% oxygen (O). Fe's element percentage was two times of Mg as expected for $MgFe_2O_4$. Oxygen element percentage was four times higher than Mg due to oxygen contribution in the activated carbon.

3.5. Characterization Composites BPAC/$MgFe_2O_4$ by Surface Area Analyzer (SAA)

The surface area of the BPAC / $MgFe_2O_4$ composite was analyzed using SAA. The results of the characterization of the surface area were 88.134 m^2/g. The surface area obtained was lower than the surface area of standard activated carbon, which has a surface area ranging from 300-3500 m^2/g [23]. The presence of $MgFe_2O_4$ crystal probably blocking the pores of activated carbon leading to the lower surface area.

The surface area of the BPAC/$MgFe_2O_4$ composite was higher than the surface area of the activated carbon of the Kepok banana peel reported by [24] of 16.53 m^2/g, higher than the surface area of nano-magnesium ferrite (n-$MgFe_2O_4$) of 53.83 m^2/g conducted by Srivastava *et al.* [25], and higher than that conducted by Rigo *et al.* [26] in a study of Nickel Ferrite/Carbon Nanotube composites with a surface area of 54 m^2/g.

3.6. Methylene Blue Adsorption Performance

3.6.1. pH Optimization of Methylene Blue

Figure 7 shows that the percentage of methylene blue adsorption by the composite BPAC/$MgFe_2O_4$ has increased from pH 5 (83.05%) and achieved optimum adsorption at pH 7 (85.03%), and then decreased again at pH 9 (80.16%). The decrease in adsorption was caused by the exchange between the adsorbent and the adsorbate. The adsorbent's surface area and the interaction between the adsorbent and the dyes determine the adsorption capacity [27].

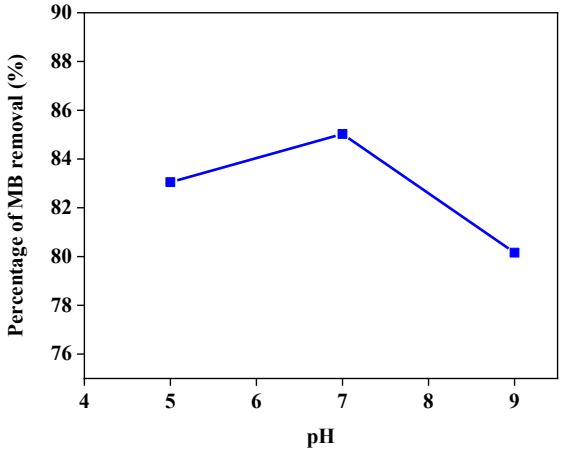

Figure 7. Percentage of MB removal in various pH

3.6.2. Result of Contact Time Variations

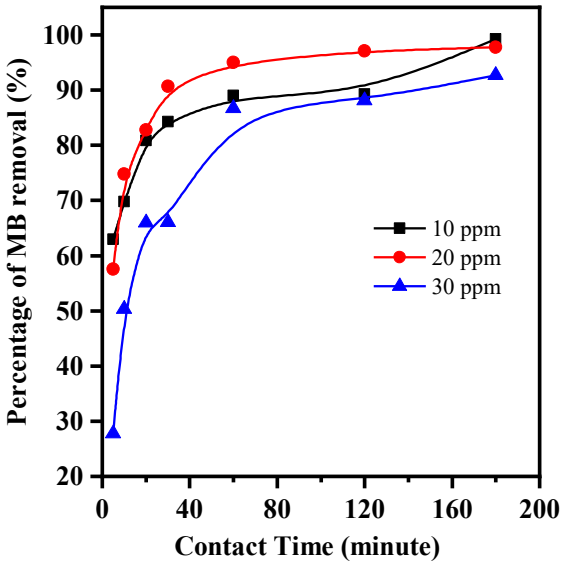

Figure 8. Methylene Blue Adsorption Percent Curve at Variation in Contact Time

Based on the results obtained in Figure 8, the longer the contact time, the more methylene blue will be adsorbed because the more chances of the adsorbent particles encountering the methylene blue dyes. This

causes more methylene blue to be bound in the adsorbent pores. The highest removal percentage was at the contact time of 180 minutes, reaching 99.26% for 10 ppm, 97.79% for a concentration of 20 ppm, and 92.65% for 30 ppm. The adsorption rate was high below 50 minutes and decelerated after 50 minutes due to the equilibrium state system.

3.6.3. Result of Concentration Variations

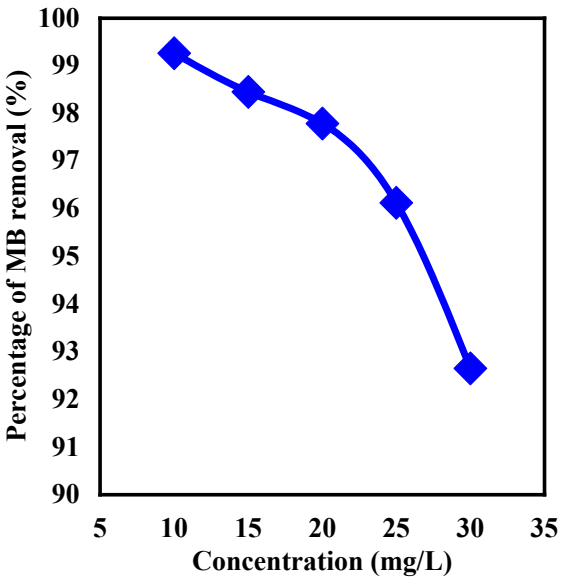

Figure 9. Methylene Blue Adsorption Percent Curve at Variation in Concentration

Based on Figure 9, The percentage of removal was not significantly changed in the range of MB concentration 10-30 ppm. Commonly, increasing the adsorbate concentration will increase the percentage of removal until it reaches maximum equilibrium adsorption capacity (q_e) and then decrease [28]. Therefore, there is an optimal concentration of adsorbate, which could not be observed yet from these data. For further observation, increasing the MB concentration range until 100 ppm perhaps will get the optimum concentration and maximum q_e.

3.7. Determination of Adsorption Isotherms

According to the mechanism, the change in adsorbate concentration in the adsorption process can be studied by determining the adsorption isotherm. The adsorption isotherm type can be used to determine the adsorbent's adsorption mechanism against the adsorbate. Liquid, solid-phase adsorption usually follows the Langmuir and Freundlich type isotherm [13]. The equation for Langmuir and Freundlich type isotherm model is shown in equation (3) and (4), respectively.

$$\frac{1}{q_e} = \frac{1}{K_L Q_m}\frac{1}{C_e} + \frac{1}{Q_m} \quad (3)$$

$$\log q_e = \left(\frac{1}{n}\right)\log C_e + \log K_F \quad (4)$$

where q_e are the adsorbate amount adsorbed per unit weight at equilibrium; C_e is the equilibrium concentration of adsorbate (mg/L); K_L is Langmuir constant; Q_m is maximum monolayer Langmuir sorption capacity; K_F is Freundlich constant, which is related to adsorption capacity (mg/g), and 1/n describes the adsorption intensity.

Determination of the type of adsorption isotherm in this study using various concentrations, namely 10, 15, 20, 25, and 30 ppm. The volume of methylene blue (adsorbate) used in the measurement was 20 mL, using 0.01 grams of BPAC/$MgFe_2O_4$ composite and 180 minutes of contact time. The linear fitting of the data to the equation (3) and (4) are shown in Figure 10a and 10b, respectively. The calculation of the adsorption isotherm model parameters is shown in Table 2.

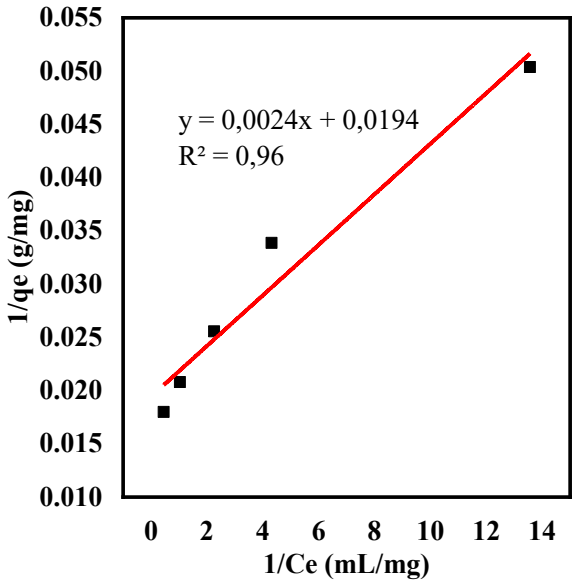

a.

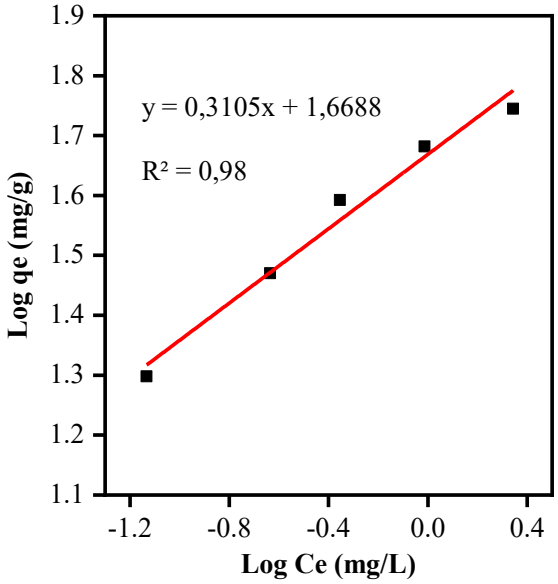

b.

Figure 10. Linear regression fitting of adsorption MB using BPAC/$MgFe_2O_4$ composite toward (a) Langmuir isotherm model and (b) Freundlich isotherm model

Table 2. Parameters of Adsorption Isotherm

Isotherm	Parameter	Value
Langmuir	Q_{max} (mg/g)	51.4
	K_L (L/mg)	8.2
	R^2	0.96
Freundlich	K_F (mg/g)	5.3
	n	3.22
	R^2	0.98

Based on Figure 10, it can be seen that the correlation coefficient (R^2) of the adsorption of methylene blue dye by the BPAC/$MgFe_2O_4$ composite shows R^2 = 0,96 for the Langmuir isotherm and the Freundlich isotherm R^2 = 0,98. The R^2 value obtained from the Freundlich isotherm model was more significant than the Langmuir isotherm model, so the adsorption that occurs tends to follow the Freundlich isotherm model, which means that the adsorption of methylene blue dye occurs physically (physical adsorption) [29].

The Q_{max} value in the Langmuir isotherm model will always be constant after reaching a particular equilibrium concentration. In the Freundlich isotherm model, the adsorption capacity increases with increasing equilibrium concentration. This indicates that the Freundlich isotherm model is not limited to single-layer adsorption so that even though the adsorbent has reached its saturation point, the adsorption process can take place at a particular stage [19]. This study's K_F value was 5.30 mg/g, more significant than the K_F carried out by [30], which was 2.85 mg/g in a study using banana peel adsorbent for methylene blue dye.

The Freundlich approach assumes that the adsorbent surface was heterogeneous, and the adsorption forms multiple (multilayer) adsorption layers that take place physically (physisorption), where each molecule has different adsorption potentials. However, the adsorbate is not firmly attached to the adsorbent. The adsorbate can move from one part of the adsorbent surface to another, and the surface left by the adsorbate can be replaced by other adsorbates [31]. This is also in accordance with the results of SEM characterization, which showed that the BPAC/$MgFe_2O_4$ composite was heterogeneous or non-uniform with irregular pores.

3.8. Determination of Adsorption Kinetics

There are two models for studying adsorption kinetics: the pseudo-first-order Lagergren model and the pseudo-second-order model [13]. The adsorption kinetics of methylene blue by BPAC/$MgFe_2O_4$ composites were evaluated based on the first-order (Eq. 5) and second-order (Eq. 6) pseudo reaction equations at variations in contact time ranging from 5 to 180 minutes and variations in concentrations of 10 ppm, 20 ppm, and 30 ppm. The linear regression fitting results are shown in Figures 11a and 11b and the result of the calculation of the adsorption kinetics constant listed in Table 3.

$$\log q_e/(q_e - q_t) = (k_1/2.303)t \quad (5)$$

$$\frac{t}{q_t} = \frac{1}{k_2 q_e^2} + \frac{1}{q_e}t \quad (6)$$

where q_t is the amount adsorbed at time t; q_e is the amount adsorbed at equilibrium; k_1 is the first-order rate equation, and k_2 is the second-order rate equation.

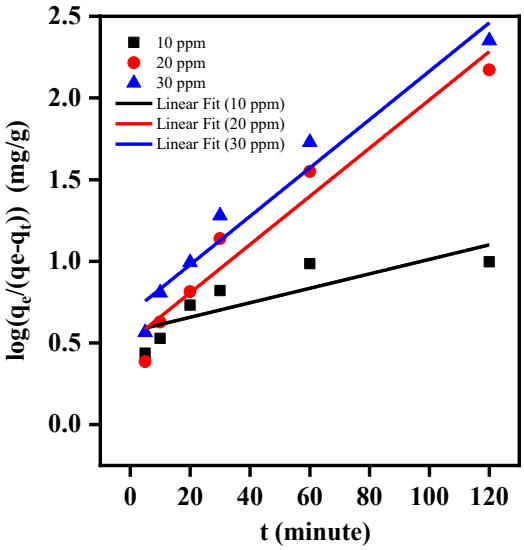

a.

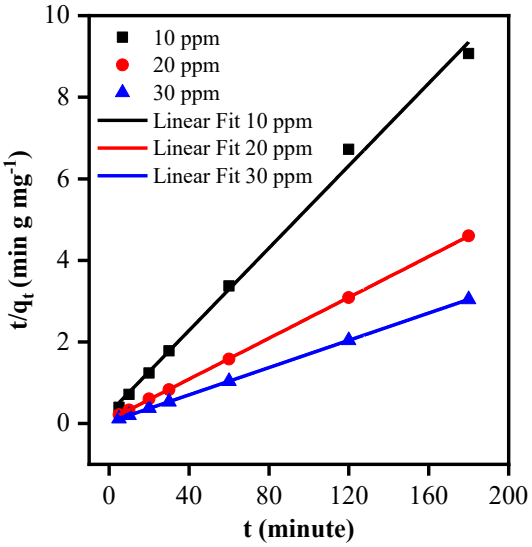

b.

Figure 11. Linear fitting regression of adsorption MB by BPAC/$MgFe_2O_4$ composite at variation concentration toward (a) pseudo-first-order and (b) pseudo-second-order equation for kinetic model

Table 3. Parameters of adsorption kinetics

Concentration (mg/L)	Adsorption Kinetics					
	Pseudo First Order			Pseudo Second Order		
	q_e (mg/g)	k_1 (min^{-1})	R^2	q_e (mg/g)	k_2 (g/mg.min)	R^2
10	3.7042	0.0101	0.6871	19.8020	0.0019	0.9960
20	3.2463	0.0064	0.9491	39.8406	0.0029	0.9996
30	4.8139	0.0042	0.9551	59.8802	0.0009	0.9999

Based Table 3 that the R^2 value in each kinetics model, at a concentration of 10 ppm, 20 ppm and 30 ppm the values were R^2 0,6871; 0,9491; 0,9551 for pseudo-first-order and R^2 value for pseudo-second-order concentrations of 10 ppm, 20 ppm and 30 ppm were 0.9960; 0.9996; 0.9999. To determine the order used, it is seen based on the R^2 value close to 1. Based on the data

obtained and shown in Table 3 of the two kinetics models, the pseudo-second-order kinetics model gives a greater R^2 than the pseudo-first-order kinetics model. It can be interpreted that the kinetics model, which is suitable to describe the adsorption kinetics model of BPAC/$MgFe_2O_4$ composites against methylene blue, was the pseudo-second-order kinetics. This kinetics model shows that the adsorption process, both adsorbent, and adsorbate influence each other's adsorption kinetics [32]. Pseudo-second-order adsorption kinetics assumes that the adsorbing capacity is proportional to the total surface adsorbent and depends on the adsorbent's ability to adsorb dyes [29]. This is consistent with the determination of the adsorption isotherm of BPAC/$MgFe_2O_4$ composites, which more closely follows the Freundlich adsorption isotherm, which states that each molecule has different adsorption potentials.

4. Conclusion

Based on the research results on making BPAC/$MgFe_2O_4$ composites as a magnetic adsorbent for methylene blue removal, it can be concluded that the preparation of BPAC/$MgFe_2O_4$ composites was successfully carried out by the coprecipitation method, the composites could adsorb methylene blue. The BPAC/$MgFe_2O_4$ composite characteristics indicated that activated carbon content was amorphous and contained Mg and Fe. The sample's surface morphology has pores with irregular shapes and heterogeneous or non-uniform characteristics. The surface area of the composites was 88.132 m^2/g. The adsorption performance of BPAC/$MgFe_2O_4$ composites showed maximum results at pH 7, 10 ppm concentration of adsorbate, and 180 minutes of contact time with a percentage of MB removal 99.26%. Furthermore, the adsorption isotherm follows the Freundlich isotherm equation with a correlation coefficient (R^2) of 0.98, with the adsorption kinetics model following the pseudo-second-order equation.

Acknowledgment

Thanks to PSTNT BATAN Bandung and LPPM Unjani Cimahi (SKEP/129/UNJANI/V/2020) for funding this research. The author also would like to thank Ms. Yofi Ike Pratiwi, Mr. Jakaria Usman, and Mr. Yamin (PSTNT, BATAN), who helped during the research process.

References

[1] Lestari Agusalim, Indonesia Agroindustry Growth Acceleration through Export Tax Policy: CGE Comparative Static Model, *Jurnal Ekonomi Kuantitatif Terapan*, 10, 2, (2017), 101-112 https://doi.org/10.24843/JEKT.2017.v10.i02.p01

[2] Octavianti Naa, Solihudin, Rubianto A. Lubis, Sintesis Komposit ZnO/Magadiit untuk Fotokatalis Zat Warna Metilen Biru dan Metil Oranye, *Seminar Nasional Sains dan Teknologi Nuklir PTNBR – BATAN* Bandung, 2013

[3] Maryam Fayazi, Mohammad Ali Taher, Daryoush Afzali, Ali Mostafavi, Enhanced Fenton-like degradation of methylene blue by magnetically activated carbon/hydrogen peroxide with hydroxylamine as Fenton enhancer, *Journal of Molecular Liquids*, 216, (2016), 781-787 https://doi.org/10.1016/j.molliq.2016.01.093

[4] Asbahani, Pemanfaatan Limbah Ampas Tebu sebagai Karbon Aktif untuk Menurunkan Kadar Besi pada Air Sumur, *Jurnal Teknik Sipil*, 13, 1, (2013), 105-114

[5] Mohamad Sobirin, Agus Yulianto, Mahardika Prasetya Aji, Efek Penambahan Karbon Aktif pada Magnetit dari Pasir Besi Sebagai Adsorpsi Ion Kalsium dalam Air, *Unnes Physics Journal*, 5, 2, (2016), 42-50

[6] Diandra Advena, Fermentasi Batang Pisang Menggunakan Probiotik dan Lama Inkubasi Berbeda terhadap Perubahan Kandungan Bahan Kering, Protein Kasar dan Serat Kasar, *undergraduate thesis*, Department of Animal Husbandry, Universitas Tamansiswa, Padang, 2014

[7] Endang Widjajanti LFX, Marfuatun, Dewi Yuanita, Pola Adsorpsi Pewarna Azo oleh Biosorben dari Kulit Pisang, *Jurnal Sains Dasar*, 2, 2, (2013), 8-16

[8] Siti Shofiah Muflihatun, Edi Suharyadi, Sintesis Nanopartikel Nickel Ferrite ($NiFe_2O_4$) dengan Metode Kopresipitasi dan Karakterisasi Sifat Kemagnetannya, *Jurnal Fisika Indonesia*, 19, 55, (2015), 20-25

[9] S. Mallesh, D. Prabu, V. Srinivas, Thermal stability and magnetic properties of $MgFe_2O_4$@ ZnO nanoparticles, *AIP Advances*, 7, 5, (2017), 056103 https://doi.org/10.1063/1.4975355

[10] P. Heidari, S. M. Masoudpanah, Structural and magnetic properties of $MgFe_2O_4$ powders synthesized by solution combustion method: the effect of fuel type, *Journal of Materials Research and Technology*, 9, 3, (2020), 4469-4475 https://doi.org/10.1016/j.jmrt.2020.02.073

[11] Agung Hermawan, Deska Lismawenning, Edi Suharyadi, Sintesis Nanopartikel Magnesium Ferrite ($MgFe_2O_4$) dengan Metode Kopresipitasi dan Karakterisasi Sifat Kemagnetannya, *Prosiding Pertemuan Ilmiah XXIX HFI Jateng & DIY*, Yogyakarta, 2015

[12] Ding Chen, Dian-yi Li, Ying-zhe zhang, Zhi-tao Kang, Preparation of magnesium ferrite nanoparticles by ultrasonic wave-assisted aqueous solution ball milling, *Ultrasonics Sonochemistry*, 20, 6, (2013), 1337-1340 https://doi.org/10.1016/j.ultsonch.2013.04.001

[13] D. Harikishore Kumar Reddy, Yeoung-Sang Yun, Spinel ferrite magnetic adsorbents: Alternative future materials for water purification?, *Coordination Chemistry Reviews*, 315, (2016), 90-111 https://doi.org/10.1016/j.ccr.2016.01.012

[14] Wenshu Tang, Yu Su, Qi Li, Shian Gao, Jian Ku Shang, Superparamagnetic magnesium ferrite nanoadsorbent for effective arsenic (III, V) removal and easy magnetic separation, *Water Research*, 47, 11, (2013), 3624-3634 https://doi.org/10.1016/j.watres.2013.04.023

[15] Yujie Huang, Yan Tang, Jun Wang, Qianwang Chen, Synthesis of $MgFe_2O_4$ nanocrystallites under mild conditions, *Materials Chemistry and Physics*, 97, 2, (2006), 394-397 https://doi.org/10.1016/j.matchemphys.2005.08.035

[16] N. Sivakumar, A. Narayanasamy, J. M. Greneche, R. Murugaraj, Y. S. Lee, Electrical and magnetic behaviour of nanostructured $MgFe_2O_4$ spinel ferrite, *Journal of Alloys and Compounds*, 504, 2, (2010), 395-402 https://doi.org/10.1016/j.jallcom.2010.05.125

[17] Vladimir Šepelák, Armin Feldhoff, Paul Heitjans, Frank Krumeich, Dirk Menzel, Fred Jochen Litterst, Ingo Bergmann, Klaus Dieter Becker, Nonequilibrium Cation Distribution, Canted Spin Arrangement, and Enhanced Magnetization in Nanosized $MgFe_2O_4$ Prepared by a One-Step Mechanochemical Route, *Chemistry of Materials*, 18, 13, (2006), 3057-3067 https://doi.org/10.1021/cm0514894

[18] Manpreet Kaur, Navneet Kaur, Kiran Jeet, Pervinder Kaur, $MgFe_2O_4$ nanoparticles loaded on activated charcoal for effective removal of Cr (VI) – A novel approach, *Ceramics International*, 41, 10, Part A, (2015), 13739-13750 https://doi.org/10.1016/j.ceramint.2015.08.040

[19] Nurhasni Nurhasni, Reski Mar'af, Hendrawati Hendrawati, Pemanfaatan Kulit Kacang Tanah (Arachis hipogaea L.) sebagai Adsorben Zat Warna Metilen Biru, *Jurnal Kimia Valensi*, 4, 2, (2018), 156-167 https://doi.org/10.15408/jkv.v4i2.8895

[20] Edi Suharyadi, Agung Hermawan, D. L. Puspitarum, Crystal Structure and Magnetic Properties of Magnesium Ferrite ($MgFe_2O_4$) Nanoparticles Synthesized by Coprecipitation Method, *Journal of Physics: Conference Series*, 1091, (2018), 012003 http://dx.doi.org/10.1088/1742-6596/1091/1/012003

[21] Arie Hardian, Fathnisa Ihsannurika Hasnah, Dani Gustaman Syarif, Senadi Budiman, Sintesis dan Karakterisasi Nanopartikel ZrO_2 dengan Metode Sol-Gel Menggunakan Amilum sebagai Capping Agent untuk Aplikasi Nanofluida, *Seminar Nasional Sains dan Teknologi Nuklir 2017*, Bandung, 2017

[22] Aflahannisa Aflahannisa, Astuti Astuti, Sintesis Nanokomposit Karbon-TiO_2 sebagai Anoda Baterai Lithium, *Jurnal Fisika Unand*, 5, 4, (2016), 357-363

[23] Siti Jamilatun, Intan Dwi Isparulita, Elza Novita Putri, Karakteristik Arang Aktif dari Tempurung Kelapa dengan Pengaktivasi H_2SO_4 Variasi Suhu dan Waktu, *CHEMICA: Jurnal Teknik Kimia*, 2, 1, (2014), 13-19 http://dx.doi.org/10.26555/chemica.v2i1.4562

[24] Antintia Sherly, Sari Edi Cahyaningrum, Aktivasi Kulit Pisang Kepok (Musa Acuminate L.) Dengan H_2SO_4 dan Aplikasinya sebagai Adsorben Ion Logam Cr(VI), *UNESA Journal of Chemistry*, 3, 1, (2014), 22-25

[25] Varsha Srivastava, Y. C. Sharma, Mika Sillanpää, Application of nano-magnesso ferrite (n-$MgFe_2O_4$) for the removal of Co^{2+} ions from synthetic wastewater: Kinetic, equilibrium and thermodynamic studies, *Applied Surface Science*, 338, (2015), 42-54 https://doi.org/10.1016/j.apsusc.2015.02.072

[26] Caroline Rigo, Eric da Cruz Severo, Marcio Antonio Mazutti, Guilherme Luiz Dotto, Sérgio Luiz Jahn, André Gündel, Márcia Maria Lucchese, Osvaldo Chiavone-Filho, Edson Luiz Foletto, Preparation of Nickel Ferrite/Carbon Nanotubes Composite by Microwave Irradiation Technique for Use as Catalyst in Photo-Fenton Reaction, *Materials Research*, 20, (2017), 311-316 https://doi.org/10.1590/1980-5373-mr-2016-0672

[27] Melyza Fitri Permanda Sari, Puji Loekitowati, Risfidian Moehadi, Penggunaan Karbon Aktif dari Ampas Tebu sebagai Adsorben Zat Warna Procion Merah dari Industri Songket, *Jurnal Pengelolaan Sumberdaya Alam dan Lingkungan*, 7, 1, (2017), 37-40 https://doi.org/10.29244/jpsl.7.1.37-40

[28] Deepak Pathania, Shikha Sharma, Pardeep Singh, Removal of methylene blue by adsorption onto activated carbon developed from Ficus carica bast, *Arabian Journal of Chemistry*, 10, (2017), S1445-S1451 https://doi.org/10.1016/j.arabjc.2013.04.021

[29] Rensy Aula Sari, M. Lutfi Firdaus, Rina Elvia, Penentuan Kesetimbangan, Termodinamika dan Kinetika Adsorpsi Arang Aktif Tempurung Kelapa Sawit Pada Zat Warna Reactive Red dan Direct Blue, *Alotrop*, 1, 1, (2017), 10-14

[30] Dyah Fitriani, Dwita Oktiarni, Lusiana, Pemanfaatan Kulit Pisang Sebagai Adsorben Zat Warna Methylene Blue, *Gradien: Jurnal Ilmiah MIPA*, 11, 2, (2015), 1091-1095

[31] Siti Zaya Aisyahlika, M. Lutfi Firdaus, Rina Elvia, Kapasitas Adsorpsi Arang Aktif Cangkang Bintaro (Cerbera odollam) terhadap Zat Warna Sintetis Reactive Red-120 dan Reactive Blue-198, *Alotrop*, 2, 2, (2018), 148-155

[32] Rifa Atul Mahmudah, Sari Edi Cahyaningrum, Penentuan Konstanta Laju Adsorpsi Ion Logam Cd(II) pada Kitosan Bead dan Kitosan-Silika Bead, *UNESA Journal of Chemistry*, 2, 1, (2013), 94-99